International Journal of Heat and Mass Transfer 52 (2009) 4807–4811

Contents lists available at ScienceDirect

International Journal of Heat and Mass Transfer

journal homepage: www.elsevier.com/locate/ijhmt

Solidification of a ternary melt from a cooled boundary, or nonlinear dynamics of mushy layers

D.V. Alexandrov *, A.A. Ivanov

Urals State University, Department of Mathematical Physics, Lenin Avenue 51, Ekaterinburg 620083, Russian Federation

ARTICLE INFO

Article history:
Received 24 February 2009
Received in revised form 7 April 2009
Accepted 28 May 2009
Available online 15 July 2009

Keywords:
Solidification
Mushy layer
Ternary alloy

ABSTRACT

We present a mathematical model and its analytical solution describing directional solidification of a ternary (three-component) system cooled from below. We focus on the solidification theory in the presence of two distinct mushy layers: (1) solidification along a liquidus surface is characterized by a primary mushy layer, and (2) solidification along a cotectic line is characterized by a secondary (cotectic) mushy layer. We consider the case when the phase transition temperatures in two mushy layers represent arbitrary functions of the compositions. We obtain an exact analytical solution of the nonlinear set of equations and boundary conditions in the case of a self-similar solidification scenario. Model predictions are in good agreement with existing experimental data.

1. Introduction

The problem of directional solidification of a solid phase from a cooled boundary comes under the rubric of so-called Stefan problems describing a wide range of physical processes [1]. Their rich nonlinear behavior has attracted substantial scientific interest and their ubiquity in fields ranging from geophysics to metallurgy stimulates developing new mathematical models and approaches. Solidification of binary solutions and melts, as an example, is rather frequently accompanied by the appearance of supercooled regions, i.e., regions in the liquid phase, the temperature of which is lower than the equilibrium temperature, which depends on the impurity concentration [2]. Due to this effect a cellular structure of the front, dendritic growth or heterogeneous nucleation can be observed [3,4]. As is evident from experimental works (see, among others, [5]), an intensive formation of dendritic structures occur for solidification of metallic melts. In this case, a large quantity of the latent heat of solidification is released in the mushy zone and, as a consequence, the constitutional supercooling completely disappears. The theoretical description of such a crystallization scenario with a quasiequilibrium mushy region was suggested for the first time in Refs. [6,7]. This nonlinear model with two moving boundaries was early solved only in particular cases of the steady-state, self-similar and arbitrary time-dependent scenarios by means of different simplifications (see, among others, [8–11]). In the opposite case, the situation changes rather drastically as a result of originating of a two-phase zone containing solid phase elements in the form of either dendrites or newly born crystals suspended in the ambient liquid. The structure of this mushy region depends, first of all, on a relation between the kinetics of both the solid phase formation and the front motion [12,13]. Many natural and industrial processes frequently met in practice cannot be explained in terms of single-component or binary systems but can be understood, at least partially, in terms of ternary systems. The present paper is devoted to a detailed analysis of a ternary alloy mushy layer model in which interfacial boundary conditions are treated explicitly. The major features of the dynamics of ternary systems can be studied using laboratory system of two salts dissolved in water, hence the mathematical model under consideration and its analytical solutions are based on laboratory experiments [14] and theoretical studies [15] where a ternary solution was cooled from below and all convection was suppressed because the buoyancy of the fluid released on crystallization always increased. The present study is concerned with new analytic results on the nonlinear dynamics of solidification of a three-component alloy with two mushy layers on the basis of experimental data on crystallization of the ternary alloy H_2O–KNO_3–$NaNO_3$.

2. The ternary phase diagram and mushy layer model

Fig. 1 illustrates a sketch of the ternary phase diagram under consideration in the spirit of Ref. [15] where all liquidus surfaces and cotectic curves are, generally speaking, nonlinear (in other words, the temperature represents an arbitrary function of the compositions along these boundaries). We denote the liquid compositions of components A, B and C by A, B and C ($A + B + C = 1$). Each of the three sides of the phase diagram describes the binary

* Corresponding author.
E-mail address: Dmitri.Alexandrov@usu.ru (D.V. Alexandrov).

0017-9310/$ - see front matter © 2009 Elsevier Ltd. All rights reserved.
doi:10.1016/j.ijheatmasstransfer.2009.05.029

Nomenclature

B and C liquid compositions of components B and C
B_∞ and C_∞ liquid compositions of components B and C far from the primary mushy layer
D_B and D_C solute diffusivities of components B and C
h_e solid phase–cotectic mushy layer boundary
h_c cotectic mushy layer–primary mushy layer boundary
h_p primary mushy layer–liquid-phase boundary
k_l and k_s thermal conductivities in the liquid and solid phases
m_B and m_C liquidus slopes
m_B^c and m_C^c cotectic slopes
n_C quadratic coefficient of the liquidus surface
n_C^c quadratic coefficient of the cotectic curve
t time
z spatial coordinate
A_E, B_E, C_E compositions of the ternary eutectic point E
B_E^{AB} composition of the B component of the binary eutectic point E_{AB}
B_{cb} and C_{cb} compositions at the cotectic mushy layer–primary mushy layer boundary
B_{pb} and C_{pb} compositions at the primary mushy layer–liquid-phase boundary
T temperature of the system
T_E temperature of the ternary eutectic point E
T_E^{AB} temperature of the binary eutectic point E_{AB}
T_M temperature of pure A
T_{pb} temperature at the primary mushy layer–liquid-phase boundary
T_0 temperature of the solid wall at $\eta = 0$
T_∞ temperature in the liquid phase far from the primary mushy layer

Greek symbols
η self-similar variable
κ thermal diffusivity in the liquid
λ_e, λ_c, λ_p dimensionless interface positions
φ_A, φ_B solid fractions of components A and B
φ_{AC}^+ and φ_{BC}^+ solid fractions of components A and B at the right side of boundary between mushy layers
φ_{AC}^- and φ_{BC}^- solid fractions of components A and B at the left side of boundary between mushy layers
φ_{AE}^+ and φ_{BC}^- solid fractions of components A and B at the right side of boundary $\eta = \lambda_e$
φ_{AE}^-, φ_{BE}^- and φ_{CE}^- solid fractions of components A, B and C at the left side of boundary $\eta = \lambda_e$

Subscripts
s solid layer
c cotectic layer
p primary layer
l liquid layer

phase diagram (T_M is the melting temperature of pure A, the binary eutectic point E_{AB} has temperature T_E^{AB} and composition B_E^{AB} of the B component). Three liquidus surfaces are formed by the binary liquidus curves along each of the three sides of the ternary phase diagram and cotectic curves extend from the binary eutectic points into the interior of the diagram (these curves are the boundaries of the liquidus surfaces). The ternary eutectic point E is located at the intersection of these curves, where the temperature is T_E and the compositions are A_E, B_E and C_E. Let a liquid-phase ternary alloy be at the point P on a liquidus surface. After cooling, component A begins to solidify out, and the components B and C are rejected into the liquid. The latter leads the system to point S on the cotectic curve. At this time, the system has a single phase transition region of the A component – primary mushy layer. When the cotectic curve is reached (point S), solidification continues and two components A and B undergo transformations in the solid state. At this time, the system goes from point S to point E along the cotectic curve. Here we have two-phase transition regions – primary and cotectic mushy layers. Thus, the curves P–S–E and S–E, respectively, correspond to the primary and primary–cotectic mushy layer solidification scenarios. Once the eutectic point E is reached, the remaining liquid solidifies to form a eutectic solid layer composed of solid A, B and C.

Let us consider the case when the phase transition temperatures in the primary and cotectic mushy layers represent arbitrary functions of the compositions B and C, i.e.,

$$T = F(B, C), \quad h_c(t) < z < h_p(t), \tag{1}$$
$$T = F_1^c(B) = F_2^c(C), \quad h_e(t) < z < h_c(t), \tag{2}$$

where h_e, h_c and h_p stand for the moving boundaries shown in Fig. 2. Functions F, F_1^c and F_2^c can be found if the temperature and compositions are known at several points of the phase diagram. Take for example the linear case [15]

$$T = T_M + m_B B + m_C C, \quad h_c(t) < z < h_p(t), \tag{3}$$
$$T = -m_B^c(B - B_E) + T_E = -m_C^c C + T_E^{AB}, \quad h_e(t) < z < h_c(t). \tag{4}$$

In this case, we need the following three points for the determination of liquidus and cotectic slopes m_B, m_C, m_B^c and m_C^c: the melting point of pure A ($B = C = 0$, $T = T_M$), the binary eutectic point for the A–B system ($B = B_E^{AB}$, $C = 0$, $T = T_E^{AB}$) and the ternary eutectic point

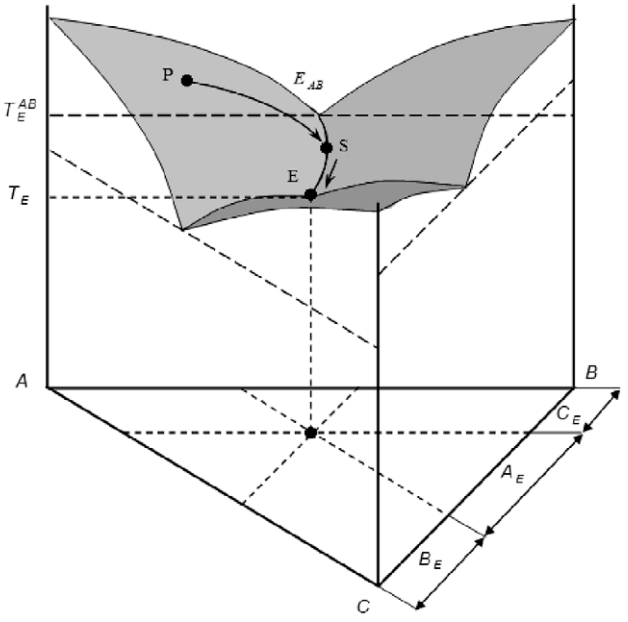

Fig. 1. The ternary phase diagram used in the model, after Anderson [15]. The three corners correspond to the pure materials A, B and C and the vertical axis corresponds to temperature.

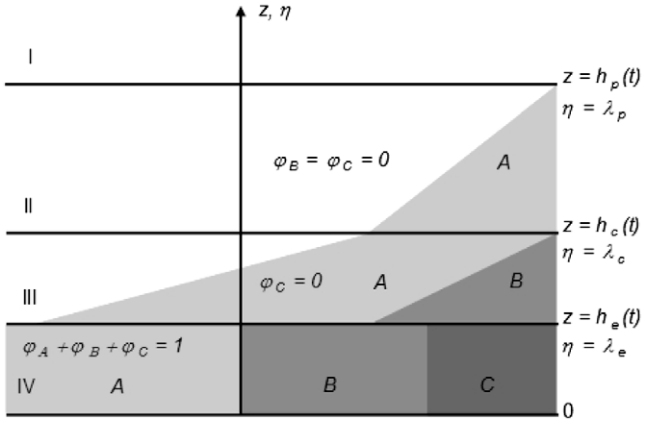

Fig. 2. Schematic diagram of solidification from a cooled boundary $z = 0$ ($\eta = 0$). The shaded regions indicate the relative proportion of each of the solid phases of components A, B and C present at each height. Regions I, II, III and IV correspond, respectively, to the liquid phase, primary mushy layer, cotectic mushy layer and solid phase; h_p, h_c and h_e represent the boundary positions (λ_p, λ_c and λ_e represent the interface positions with respect to the similarity variable η).

($B = B_E$, $C = C_E$, $T = T_E$). Substitution of these points into expressions (3) and (4) gives $m_B = (T_E^{AB} - T_M)/B_E^{AB}$, $m_C = -m_C^c(1 + m_B/m_B^c)$, $m_B^c = (T_E^{AB} - T_E)/(B_E - B_E^{AB})$, $m_C^c = (T_E^{AB} - T_E)/C_E$. It is obvious that in general case we need more known points for the determination of F, F_1^c and F_2^c.

Let us treat the solidification process as self-similar (see experiments [14]). What this means is positions of all boundaries are directly proportional to the square root of time. Therefore, we introduce interface positions and self-similar variable η of the form

$$h_e(t) = 2\lambda_e\sqrt{\kappa t}, \quad h_c(t) = 2\lambda_c\sqrt{\kappa t}, \quad h_p(t) = 2\lambda_p\sqrt{\kappa t}, \tag{5}$$

$$\eta = \frac{z}{2\sqrt{\kappa t}}. \tag{6}$$

Here λ_e, λ_c and λ_p are dimensionless interface positions to be determined.

In the liquid layer ($\eta > \lambda_p$) the temperature distribution can be expressed in terms of the complementary error function

$$T_l(\eta) = T_\infty + (T_{pb} - T_\infty)\frac{erfc(\eta)}{erfc(\lambda_p)} \tag{7}$$

while the compositions are practically constants in accordance with experiments of Ref. [14].

Taking into account that relaxation times of the concentration fields are several orders of magnitude high than the thermal relaxation time, the temperature field in mushy layers can be regarded as linear function of η (see also [14]). Also, experiments [14] show that the concentration fields in mushy layers are nearly linear. The latter leads us to the Scheil form of these equations [16,17]. How to solve the diffusion equations in the general form is discussed in Ref. [18]. However, for the sake of simplicity, we use here their analogs in the Scheil form in accordance with Ref. [15]

$$\frac{\partial}{\partial t}((1-\varphi_A)B) = 0 \quad ,\frac{\partial}{\partial t}((1-\varphi_A)C) = 0, \quad h_c(t) < z < h_p(t),$$
$$\frac{\partial}{\partial t}((1-\varphi_A-\varphi_B)B + \varphi_B) = 0, \quad \frac{\partial}{\partial t}((1-\varphi_A-\varphi_B)C) = 0,$$
$$h_e(t) < z < h_c(t)$$

Thus, the temperature and compositions can be written in the form

$$T_p(\eta) = T_1 + \eta T_2 = F(B, C), \tag{8}$$

$$B(\eta) = \frac{B_{pb}}{1-\varphi_A(\eta)}, \quad C(\eta) = \frac{C_{pb}}{1-\varphi_A(\eta)} \tag{9}$$

in the primary mushy layer $\lambda_c < \eta < \lambda_p$ and

$$T_c(\eta) = T_3 + \eta T_4 = F_1^c(B) = F_2^c(C), \tag{10}$$

$$B(\eta) = \frac{B_{cb}(1-\varphi_{\bar{AC}}-\varphi_{\bar{BC}}) + \varphi_{\bar{BC}} - \varphi_B(\eta)}{1-\varphi_A(\eta)-\varphi_B(\eta)}, \tag{11}$$

$$C(\eta) = \frac{C_{cb}(1-\varphi_{\bar{AC}}-\varphi_{\bar{BC}})}{1-\varphi_A(\eta)-\varphi_B(\eta)} \tag{12}$$

in the cotectic mushy layer $\lambda_e < \eta < \lambda_c$.

In the solid phase, $0 < \eta < \lambda_e$, the temperature is also nearly linear function of η

$$T_s(\eta) = T_0 + \frac{T_E - T_0}{\lambda_e}\eta. \tag{13}$$

The boundary conditions on the liquid–primary mushy layer interface $\eta = \lambda_p$ written by means of the self-similar variables (5) and (6) are given by

$$T_l = T_p = T_{pb} = F(B_{pb}, C_{pb}), \tag{14}$$

$$\frac{dT_l}{d\eta} = \frac{dT_p}{d\eta}, \quad \varphi_A = 0, \tag{15}$$

$$2\kappa\lambda_p(B_{pb} - B_\infty) = -D_B\frac{dB}{d\eta}, \quad 2\kappa\lambda_p(C_{pb} - C_\infty) = -D_C\frac{dC}{d\eta}, \tag{16}$$

where we consider the commonly occurring case $\varphi_A = 0$ at $\eta = \lambda_p$ [9]. The last boundary conditions describe nearly constant distributions of the compositions B and C in the liquid. Here T_{pb}, B_{pb}, C_{pb}, B_{cb}, C_{cb}, T_1, T_2, T_3, T_4, $\varphi_{\bar{AC}}$, $\varphi_{\bar{BC}}$ are parameters to be determined.

Combining expressions (8) and (14), we find T_1 and T_{pb}

$$T_1 = F(B_{pb}, C_{pb}) - \lambda_p T_2, \quad T_{pb} = F(B_{pb}, C_{pb}). \tag{17}$$

Taking the derivatives of expressions (9) with respect to η

$$\frac{dB}{d\eta} = \frac{B_{pb}}{(1-\varphi_A)^2}\frac{d\varphi_A}{d\eta}, \quad \frac{dC}{d\eta} = \frac{C_{pb}}{(1-\varphi_A)^2}\frac{d\varphi_A}{d\eta} \tag{18}$$

and substituting the result into the boundary conditions (16), we obtain C_{pb} in terms of B_{pb}

$$C_{pb} = \frac{DB_{pb}C_\infty}{B_{pb}(D-1) + B_\infty}, \quad D = \frac{D_B}{D_C}. \tag{19}$$

Eqs. (8) and (9) determine the solid fraction $\varphi_A(\eta)$ in the primary mushy layer in terms of its inverse function

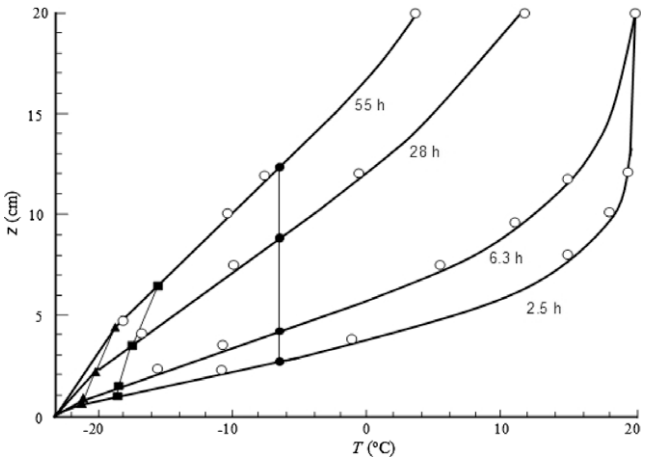

Fig. 3. Temperature profiles calculated at various times (numbers at the curves). Open circles show experimental data ([14], experiment 7). Overlain are the positions of the mush–liquid interface (dark circles), the cotectic front (dark squares) and the eutectic front (dark triangles).

$$T_1+\eta T_2=F\left(\frac{B_{pb}}{1-\varphi_A},\frac{C_{pb}}{1-\varphi_A}\right)\equiv G(\varphi_A); \tag{20}$$

whence

$$\frac{d\varphi_A}{d\eta}=T_2\left(\frac{dG}{d\varphi_A}\right)^{-1}.$$

Now, substitution of (18) in (16) at $\varphi_A=0$ gives T_2 in the form

$$T_2=\frac{2\kappa\lambda_p(B_\infty-B_{pb})}{D_B B_{pb}}\left(\frac{dG}{d\varphi_A}\right)_{\varphi_A=0}. \tag{21}$$

Furthermore, combining expressions (7), (8), (15), and (21), we come to the following equation for the determination of two unknowns B_{pb} and λ_p

$$\frac{(T_\infty-G(0))D_B B_{pb}}{\sqrt{\pi}\kappa}=\lambda_p(B_\infty-B_{pb})erfc(\lambda_p)\exp(\lambda_p^2)\left(\frac{dG}{d\varphi_A}\right)_{\varphi_A=0}. \tag{22}$$

The second equation connecting these values will be found below.

Substituting $\eta=\lambda_c$ and $\varphi_A=\varphi_{AC}^+$ into (20) and using (17) one can get the primary mushy layer–cotectic mushy layer interface position

$$\lambda_c=\lambda_p+\frac{1}{T_2}\left[F\left(\frac{B_{pb}}{1-\varphi_{AC}^+},\frac{C_{pb}}{1-\varphi_{AC}^+}\right)-G(0)\right]. \tag{23}$$

Continuity equations for the temperature and compositions on the primary mushy layer–cotectic mushy layer interface $\eta=\lambda_c$ have the form

$$T_p=T_c,\quad \frac{B_{pb}}{1-\varphi_{AC}^+}=B_{cb},\quad \frac{C_{pb}}{1-\varphi_{AC}^+}=C_{cb},\quad \varphi_{BC}^+=0. \tag{24}$$

Substitution of (8) and (10) in (24) gives T_3, C_{cb} and φ_{AC}^+ in the form

$$T_3=T_1+\lambda_c(T_2-T_4),\quad C_{cb}=B_{cb}\frac{C_{pb}}{B_{pb}},\quad \varphi_{AC}^+=1-\frac{B_{pb}}{B_{cb}}. \tag{25}$$

Also, expressions (8) and (10) at $\eta=\lambda_c$ lead to the following equation for $B_{cb}=B_{cb}(B_{pb})$

$$F\left(B_{cb},\frac{C_{pb}}{B_{pb}}B_{cb}\right)=F_1^c(B_{cb}). \tag{26}$$

The boundary conditions at $\eta=\lambda_c$ connecting the thermal and diffusion fluxes and the rate of interface motion dh_c/dt written by means of the self-similar variables (5) and (6) have the form (see [15])

$$2\lambda_c\kappa L_V(\varphi_{AC}^+-\varphi_{AC}^--\varphi_{BC}^-)=[(1-\varphi_{AC}^+)k_l+\varphi_{AC}^+k_s]T_2-[(1-\varphi_{AC}^--\varphi_{BC}^-)\times k_l+(\varphi_{AC}^-+\varphi_{BC}^-)k_s]T_4, \tag{27}$$

$$\frac{2\lambda_c\kappa}{D_B}[B_{cb}(\varphi_{AC}^+-\varphi_{AC}^-)+(1-B_{cb})\varphi_{BC}^-]=B_{cb}T_2\left(\frac{dG}{d\varphi_A}\right)_{\varphi_{AC}^+}^{-1}-(1-\varphi_{AC}^--\varphi_{BC}^-)T_4\left(\frac{dF_1^c}{dB}\right)_{B_{CB}}^{-1}, \tag{28}$$

$$\frac{2\lambda_c\kappa}{D_c}C_{cb}(\varphi_{AC}^+-\varphi_{AC}^--\varphi_{BC}^-)=C_{cb}T_2\left(\frac{dG}{d\varphi_A}\right)_{\varphi_{AC}^+}^{-1}-(1-\varphi_{AC}^--\varphi_{BC}^-)T_4\left(\frac{dF_2^c}{dC}\right)_{C_{CB}}^{-1}, \tag{29}$$

where we use

$$\frac{dB}{d\eta}=T_4\left(\frac{dF_1^c}{dB}\right)^{-1},\quad \frac{dC}{d\eta}=T_4\left(\frac{dF_2^c}{dC}\right)^{-1}.$$

It is an easy matter to express φ_{AC}^-, φ_{BC}^- and T_4 from Eqs. (27)–(29) dependent of two unknowns dh_c/dt and λ_p. However, we will not dwell on this point to save room. Now, the solid fractions $\varphi_A(\eta)$ and $\varphi_B(\eta)$ distributed in the cotectic mushy layer can be easily found from Eqs. (10)–(12). Furthermore, equating temperature (10) at $\eta=\lambda_e$ to the known temperature of the ternary eutectic point E, we come to three equations for the determination of φ_{AE}^+, φ_{BE}^+ and λ_e; for instance, for λ_e, we have

$$\lambda_e=\frac{T_E-T_3}{T_4}. \tag{30}$$

The solid fractions φ_{AE}^-, φ_{BE}^- and φ_{CE}^- at the left side of boundary $\eta=\lambda_e$ can be found from the mass balance conditions written by means of the self-similar variables (5) and (6) [15]

$$\varphi_{BE}^-=\frac{D_B}{2\lambda_e\kappa}(1-\varphi_{AE}^+-\varphi_{BE}^+)T_4\left(\frac{dF_1^c}{dB}\right)_{B_E}^{-1}-B_E(\varphi_{AE}^++\varphi_{BE}^+-1)+\varphi_{BE}^+, \tag{31}$$

$$\varphi_{CE}^-=\frac{D_C}{2\lambda_e\kappa}(1-\varphi_{AE}^+-\varphi_{BE}^+)T_4\left(\frac{dF_2^c}{dC}\right)_{C_E}^{-1}-C_E(\varphi_{AE}^++\varphi_{BE}^+-1), \tag{32}$$

$$\varphi_{AE}^-=1-\varphi_{BE}^--\varphi_{CE}^-.$$

In order to obtain the second equation for B_{pb} and λ_p, we use the balance condition for heat fluxes imposed at the solid phase–cotectic mushy layer interface (see, for example, [15])

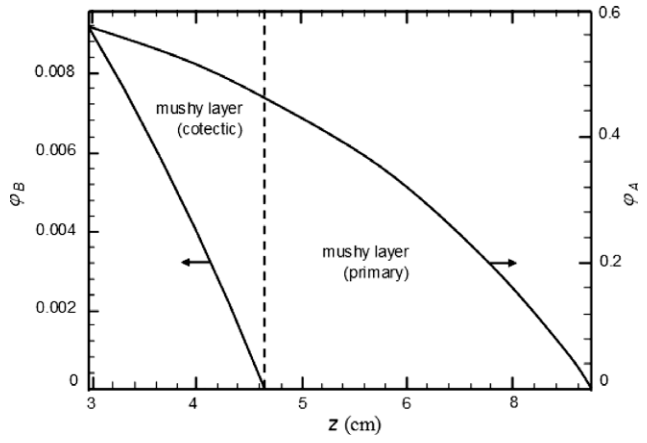

Fig. 4. The solid fractions in mushy layers as functions of the spatial coordinate at $t=10^5$ s.

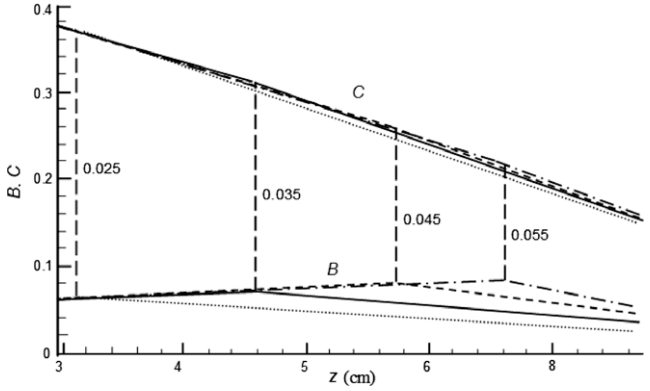

Fig. 5. The concentrations in the residual liquid as functions of the dimensional coordinate at $t=10^5$ s ($B_\infty=0.025$ – dotted lines, $B_\infty=0.035$ – solid lines, $B_\infty=0.045$ – dashed lines and $B_\infty=0.055$ – chain-dotted lines). Vertical lines show the cotectic front at various values of B_∞ (numbers at the lines), whereas the boundary positions of interfaces $h_e\approx 2.94$ cm and $h_p\approx 8.7$ cm are practically unchanged for calculated variations of B_∞.

$$2\lambda_e \kappa L_V(\varphi^+_{AE}+\varphi^+_{BE}-1)=T_4\left[(1-\varphi^+_{AE}-\varphi^+_{BE})k_l +(\varphi^+_{AE}+\varphi^+_{BE})k_s-\frac{T_E-T_0}{T_E-T_3}k_s\right]. \quad (33)$$

Now, two unknowns B_{pb} and λ_p can be calculated from Eqs. (22) and (33), whereas all the rest parameters describing the process under consideration can be found from expressions (8)–(13), (17)–(21) and (27)–(32) by substitution of B_{pb} and λ_p.

To take into account possible deviations of the phase transition temperatures from linear dependences (3) and (4), we will use their quadratic analogs. However, by virtue of the fact that the main contribution is connected with component C ([14], experiment 7), one can use the following approximations

$$T_p = T_M + m_B B + m_C C + n_C C^2, \quad h_c(t) < z < h_p(t),$$
$$T_c = -m^c_B(B-B_E)+T_E = -m^c_C C + n^c_C C^2 + T^{AB}_E, \quad h_e(t) < z < h_c(t).$$

In this case, as before, we have three points for the determination of liquidus and cotectic slopes m_B, m_C, m^c_B and m^c_C. In order to find quadratic coefficients n_C and n^c_C, we know from experiments [14] that the interface temperature T^* between the liquid phase and primary mushy layer is practically unchanged ($T_* \approx -6.3\,^\circ$C). Using the latter, and omitting trivial mathematical manipulations, we ultimately arrive at

$$m_B=\frac{T^{AB}_E-T_M}{B^{AB}_E}, \quad m_C=\frac{T_E-T_M-m_B B_E-n_C C^2_E}{C_E},$$
$$m^c_B=\frac{T^{AB}_E-T_E}{B_E-B^{AB}_E}, \quad m^c_C=\frac{T^{AB}_E-T_E+n^c_C C^2_E}{C_E},$$
$$n_C=\frac{1}{C_\infty(C_\infty-C_E)}\left[T_*-T_M-m_B B_\infty-(T_E-T_M-m_B B_E)\frac{C_\infty}{C_E}\right],$$
$$n^c_C=\frac{B^2_\infty}{B_{cb}C_\infty(B_{cb}C_\infty-C_E B_\infty)}\left[T_M+m_B B_{cb}+m_C B_{cb}\frac{C_\infty}{B_\infty} + n_C B^2_{cb}\frac{C^2_\infty}{B^2_\infty}+\frac{B_{cb}C_\infty}{C_E B_\infty}(T^{AB}_E-T_E)-T^{AB}_E\right].$$

In the general case, we need more measured points for the determination of functions (1) and (2).

3. Discussion

Figs. 3–5 illustrate various distributions in accordance with the theory under consideration for the system H_2O–KNO_3–$NaNO_3$ provided by the experimental work [14] (thermophysical properties of the system are given by Anderson [15] in Table 1, experiment 7). Fig. 3 shows the temperature profiles in all regions for fixed values of the solidification time. It is interesting to note that the mush–liquid interface has an approximately constant temperature as predicted previously by experiments [14]. Apparently, this is due to the fact that the mush–liquid interface has a temperature close to the equilibrium liquidus temperature. Also, the latter is consistent with the constant concentrations in the liquid phase connected with temperature T_{pb} by Eq. (1). The temperatures of the other two interfaces increase with time because of the constitutional supercooling. As may be seen from Fig. 4, the solid fractions in two mushy layers decrease away from the boundary solid phase–cotectic mushy layer. Such a behavior corresponds to the classical solidification theory of binary mixtures (see, among others, [12]). Fig. 5 demonstrates a behavior of the compositions in the cotectic and primary mushy layer. As would be expected, the liquid composition C decreases with z due to the effect of impurity displacement by the growing crystal. Contrary to this classical behavior, the liquid composition B increases (decreases) with z in the cotectic (primary) layer. The liquid composition B attains its maximum at the moving phase transition interface between cotectic and primary mushy layers. From the mathematical point of view, this is due to the fact that coefficients m_B, m_C and m^c_B are negative (see, for example, expressions (4)). Physically, the reason is that the liquid composition B undergoes a phase transition in the cotectic mushy layer resulting in a decreasing of composition B in the vicinity of the phase transition interface $h_e(t)$. Also, an important point is that the cotectic (primary) mushy layer thickness increases (decreases) with increasing composition B (with increasing impurity of the second component of a ternary alloy). In other words, this underlines the role of two different phase transition layers as the compositions vary.

Acknowledgments

This work was made possible due to the financial support of Grant Nos. 08-01-00298, 09-08-00844, 07-03-96069 Ural, 07-01-33596091 Ural (Russian Foundation for Basic Research), 2.1.1/336 2571 (Ministry of Education) and 02.740.11.0202 (Federal Target Program).

References

[1] A.M. Meirmanov, The Stefan Problem, De Gruyter, Berlin, 1992.
[2] G.P. Ivantsov, Diffusive supercooling in binary alloy solidification, Dokl. Akad. Nauk SSSR 81 (1951) 179–182.
[3] M. Flemings, Solidification Processing, McGraw Hill, New York, 1974.
[4] B. Chalmers, Principles of Solidification, Wiley, New York, 1964.
[5] V.T. Borisov, Yu.E. Matveev, Determination of temperature at the beginning of mushy region of binary melts (short letter), Fiz. Met. Metalloved. 13 (3) (1962) 465–467.
[6] V.T. Borisov, Theory of Two-Phase Zone of Metallic Ingot, Metallurgia, Moscow, 1987.
[7] R.N. Hills, D.E. Loper, P.H. Roberts, A thermodynamically consistent model of a mushy zone, Q. J. Appl. Math. 36 (1983) 505–539.
[8] D.V. Alexandrov, Solidification with a quasiequilibrium mushy region: exact analytical solution of nonlinear model, J. Cryst. Growth 22 (2001) 816–821.
[9] D.V. Alexandrov, A.P. Malygin, Self-similar solidification of an alloy from a cooled boundary, Int. J. Heat Mass Transfer 49 (2006) 763–769.
[10] D.V. Alexandrov, A.P. Malygin, I.V. Alexandrova, Solidification of leads: approximate solutions of non-linear problem, Ann. Glaciol. 44 (2006) 118–122.
[11] D.V. Alexandrov, I.G. Nizovtseva, To the theory of underwater ice evolution, or nonlinear dynamics of false bottoms, Int. J. Heat Mass Transfer 51 (2008) 5204–5208.
[12] Yu.A. Buyevich, D.V. Alexandrov, V.V. Mansurov, Macrokinetics of Crystallization, Begell House, New York and Wallingford, 2001.
[13] D.L. Aseev, D.V. Alexandrov, Directional solidification of binary melts with a non-equilibrium mushy layer, Int. J. Heat Mass Transfer 49 (2006) 4903–4909.
[14] A. Aitta, H.E. Huppert, M.G. Worster, Diffusion-controlled solidification of a ternary melt from a cooled boundary, J. Fluid Mech. 432 (2001) 201–217.
[15] D.M. Anderson, A model for diffusion-controlled solidification of ternary alloys in mushy layers, J. Fluid Mech. 483 (2003) 165–197.
[16] E. Scheil, Bemerkungen zur schichtkiistallbildung, Z. Metallkd. 34 (1942) 70–72.
[17] R.C. Kerr, A.W. Woods, M.G. Worster, H.E. Huppert, Solidification of an alloy cooled from above: Part 1. Equilibrium growth, J. Fluid Mech. 216 (1990) 323–342.
[18] D.V. Alexandrov, Nonlinear dynamics of solidification in three-component systems, Dokl. Phys. 53 (9) (2008) 471–475.